Available online at www.sciencedirect.com
ScienceDirect
Journal of Sound and Vibration 307 (2007) 280–294
JOURNAL OF SOUND AND VIBRATION
www.elsevier.com/locate/jsvi

Approaches to estimating the reflection and transmission coefficients of discontinuities in waveguides from measured data

J.M. Muggleton*, T.P. Waters, B.R. Mace, B. Zhang

Institute of Sound and Vibration Research, University of Southampton, Highfield, Southampton SO17 1BJ, UK

Received 21 February 2007; received in revised form 4 July 2007; accepted 4 July 2007

Abstract

The vibration modelling of waveguides is relevant to many engineering applications. Although there are many prediction techniques available, at present a fundamental weakness can undermine all of them; this weakness arises from inadequate modelling of joints and discontinuities due to uncertainty in joint properties and behaviour. An approach to joint parameter estimation from vibration measurements, which makes use of wave models of waveguide systems, has been proposed previously. In this paper, a number of approaches to estimating the reflection and transmission coefficients of a joint from measured data are developed. Of particular interest is the case where only a limited set of measured data is available. Initially a generalized joint in a waveguide system, which may support many wavetypes, is considered. Further insights into the behaviour of such a system are then gained by examining a much simpler system in which only one wavetype can exist. Finally, measurements are made on a beam with a mass/moment of inertia discontinuity and on a pipe with a right-angled bend, both with flexural excitation, in order to demonstrate the procedures and to highlight some of the inherent difficulties.

1. Introduction

Reducing the transmission of structure-borne noise and vibration from built-up structures can be a challenging problem. Many structural components can be regarded as waveguides, unintentionally conveying vibrational energy away from the source of excitation via wave propagation through the structure [1–4]. Sound radiation from these components and, more generally, the infrastructure to which the components are connected is an annoyance and can become a health and safety issue. Many installations occur in safety critical applications where structural integrity is paramount. Dynamic modelling of systems will often be required to determine typical in-operation stress cycles for fatigue predictions, and such a model may also be used in combination with vibration measurements to estimate changes in the system with time.

Currently available prediction techniques for vibration achieve different compromises between the conflicting demands of accuracy and complexity. In general, there is no ideal technique and there is a case for developing continuous models to accommodate more complex configurations. Improved techniques are required that can model built-up structures whilst retaining a physical insight into vibration behaviour.

*Corresponding author.
E-mail address: jm9@soton.ac.uk (J.M. Muggleton).

0022-460X/$ - see front matter © 2007 Elsevier Ltd. All rights reserved.
doi:10.1016/j.jsv.2007.07.007

Irrespective of the method adopted, however, modelling can be undermined by uncertainty in the parameters of the structural model, particularly in the joints [5,6]. Built-up systems often comprise many joints; in pipe systems, for example, these can be in the form of flanges, hangers, pumps and changes in section. Dynamically, these joints contribute stiffness, inertia and damping and can dramatically alter the response of the system. Frequently, the inertia is modelled explicitly but the joint is assumed to be perfectly rigid [7,8]; alternatively stiffness can be incorporated by using discrete elements [9,10]. Damping can be chosen for reasons of convenience by a complex Young's modulus, the use of discrete elements, measured modal damping values, or omitted altogether (see for example Ref. [9]). Alternatively, joint properties can be estimated from vibration measurements [11–15].

The joint properties can be parametrically determined in a number of ways. One possibility, and that which motivates the work described here, is to measure the reflection and transmission coefficients for the joint in question and then to use a wave model to infer the dynamic characteristics of the joint. Measuring reflection and transmission coefficients on a system in which only one wave type is present is a relatively simple matter, particularly if the system can be considered to be semi-infinite either side of the joint. However, when the system is finite and there is more than one wave type present, the situation becomes more complex.

In this paper, a number approaches to estimating the reflection and transmission coefficients of a joint in a finite waveguide system from measured data are developed. Of particular interest is the case where only a limited set of measured data is available. The theoretical basis for the approaches is discussed with reference to a generalized joint in a waveguide system which may support many wavetypes. Further insights into the behaviour of such a system are then gained by examining a much simpler system in which only one wavetype can exist. In this case the effects of the joint and any reflections from the system boundaries can be seen explicitly and, in certain circumstances, effectively separated.

Measurements are made on a beam with a mass/inertia discontinuity and on a pipe with a right-angled bend, both undergoing flexural excitation, in order to demonstrate the procedures and to highlight some of the inherent difficulties. For the beam, only flexural waves are supported, whilst for the pipe, flexural, axial, and torsional waves can exist. For each set of measurements, estimates are made of the reflection and transmission coefficients of the discontinuity using the proposed methods. The coefficients are then compared with predictions from simple wave models of each discontinuity.

2. Theoretical framework

2.1. General case

Consider a discontinuity in a waveguide structure. The discontinuity might be an attachment or a junction of two or more waveguides; for pipe networks it might be a bend, a hanger or a change in section. The incoming and outgoing waves $\boldsymbol{\phi}_{\text{in}}$ and $\boldsymbol{\phi}_{\text{out}}$ are related by

$$\boldsymbol{\phi}_{\text{out}} = \mathbf{S}\boldsymbol{\phi}_{\text{in}}, \tag{1}$$

where $\mathbf{S}$ is a scattering matrix. There may be any number of waveguides at the discontinuity and each waveguide can support a number of different wave types (bending, torsion, axial, etc.). For the case of two waveguides A and B shown in Fig. 1 then

$$\boldsymbol{\phi}_{\text{in}} = \begin{Bmatrix} \mathbf{a}^{+} \\ \mathbf{b}^{-} \end{Bmatrix}, \quad \boldsymbol{\phi}_{\text{out}} = \begin{Bmatrix} \mathbf{a}^{-} \\ \mathbf{b}^{+} \end{Bmatrix}, \quad \mathbf{S} = \begin{bmatrix} \mathbf{R}_{aa} & \mathbf{T}_{ab} \\ \mathbf{T}_{ba} & \mathbf{R}_{bb} \end{bmatrix}, \tag{2a–c}$$

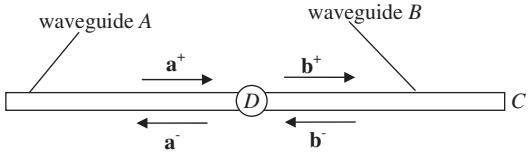

Fig. 1. Two waveguides with a discontinuity.

where $\mathbf{R}$ and $\mathbf{T}$ are matrices of reflection and transmission coefficients. Various relations hold between the elements of these matrices because of reciprocity, conservation of energy and symmetry [16]. At this stage, no assumptions have been made as to how the waveguides A and B might be terminated.

The aim is to measure at least some of the elements of $\mathbf{S}$. In practice the magnitudes of the reflection and transmission coefficients will often be of most interest. In general, one might excite the structure, measure all the wave amplitudes, repeat the experiment a sufficient number of times and concatenate the results to provide the estimate

$$\widehat{\mathbf{S}} = \mathbf{\Phi}_{\text{out}}\mathbf{\Phi}_{\text{in}}^{-1}, \tag{3}$$

where

$$\mathbf{\Phi} = [\boldsymbol{\phi}_1 \quad \boldsymbol{\phi}_2 \quad \dots \quad \boldsymbol{\phi}_n] \tag{4}$$

and where $\boldsymbol{\phi}_k$ is the vector of wave amplitudes for the kth experiment. This approach is typically impractical and hence alternative, approximate solutions are sought.

Firstly, suppose that the structure is anechoic at both ends so that the outgoing waves are not reflected back towards the discontinuity. If, for a single experiment, only the jth incoming wave $\phi_{\text{in},\,j}$ is excited and the jth and ith incoming and outgoing wave amplitudes are measured, then the (i, j)th element of $\mathbf{S}$ is

$$S_{ij} = \phi_{\text{out},i}/\phi_{\text{in},j}. \tag{5}$$

Thus the elements can be measured one-by-one.

Suppose, on the other hand, that the structure is not anechoic at either end. The outgoing waves are reflected back towards the discontinuity by boundaries and the like which are described by some reflection matrix $\mathbf{R}_E$. Suppose that incoming waves $\boldsymbol{\phi}_e$ are excited directly. The total waves incident on the discontinuity are therefore

$$\boldsymbol{\phi}_{\text{in}} = \boldsymbol{\phi}_e + \mathbf{R}_E\boldsymbol{\phi}_{\text{out}}. \tag{6}$$

From Eq. (1)

$$\phi_{\text{out},i} = S_{ij}\phi_{\text{in},j} + \sum_{m\neq j} S_{im}\phi_{\text{in},m}. \tag{7}$$

The anechoic formulation, $\phi_{\text{out},\,i}/\phi_{in,\,j}$ given in Eq. (5) now no longer gives the required scattering matrix, S_{ij}, but gives an estimate, $\hat{S}_{ij}$, which will also contain additional terms

$$\widehat{S}_{ij} = \frac{\phi_{\text{out},i}}{\phi_{\text{in},j}} = S_{ij} + \sum_{m\neq j} S_{im}\frac{\phi_{\text{in},m}}{\phi_{\text{in},j}}. \tag{8}$$

These additional terms might arise in $\boldsymbol{\phi}_e$ from inadvertently excited waves or by wave mode conversion of excited waves subsequently reflected at the boundaries. They also arise because of wave mode conversion in the reflections of the outgoing waves (the term $\mathbf{R}_E\boldsymbol{\phi}_{\text{out}}$ in Eq. (6)). There are also measured outgoing waves which arise from unmeasured incident waves—the last term on the right-hand side of Eq. (7). From Eqs. (1) and (6) it follows that

$$\boldsymbol{\phi}_{\text{in}} = [\mathbf{I} - \mathbf{R}_E\mathbf{S}]^{-1}\boldsymbol{\phi}_e. \tag{9}$$

The matrix inversion in Eq. (9), which encapsulates resonant behaviour in the structure, tends to bias the anechoic estimate because certain frequency components might be preferentially amplified. Clearly the general situation is extremely complicated, but insights into the behaviour of such systems can be gleaned by examining a more simple system in which only one wavetype is present. Under certain circumstances, these insights can then be exploited to achieve better estimates from a limited data set. This is discussed in more detail below.

2.2. A simplified discontinuity

In this section, a generalized discontinuity in a one-dimensional (1D) finite system is considered. For simplicity, it is assumed at this stage that only one propagating wavetype can exist in the system. The system is very similar to that depicted in Fig. 1, except that here, the waves in each waveguide are scalar quantities. Furthermore, waveguide B terminates at C with a complex reflection coefficient of $R\,\mathrm{e}^{\mathrm{i}\varepsilon}$. Waveguide A may either be semi-infinite or terminated at some boundary.

Waves can propagate in each waveguide in both positive and negative x-directions. For any excitation, the wave amplitudes at the discontinuity are related by

$$\begin{bmatrix} a^- \\ b^+ \end{bmatrix} = \begin{bmatrix} r\,\mathrm{e}^{\mathrm{i}\alpha} & t\,\mathrm{e}^{\mathrm{i}\beta} \\ t\,\mathrm{e}^{\mathrm{i}\beta} & r\,\mathrm{e}^{\mathrm{i}\alpha} \end{bmatrix} \begin{bmatrix} a^+ \\ b^- \end{bmatrix}, \tag{10}$$

where $r\,\mathrm{e}^{\mathrm{i}\alpha}$ and $t\,\mathrm{e}^{\mathrm{i}\beta}$ are the complex reflection and transmission coefficients of the discontinuity (assumed to be symmetrical, so that the reflection and transmission coefficients are independent of whether the incident wave impinges on the joint from waveguide A or waveguide B, and the discontinuity can be characterized by two complex coefficients only).

If the system of waves arises from some external excitation at frequency ω of waveguide A (i.e. there is no external excitation of waveguide B), the waves in B can be simply related via the reflection coefficient at C and a propagation term, viz.,

$$b^- = R\,e^{\mathrm{i}(\varepsilon-2kl)}b^+, \tag{11}$$

where k is the wavenumber for the waves at that frequency and l is the length of B.

The reflected wave at the discontinuity in waveguide A, a^-, and the transmitted wave at the discontinuity in B, b^+, can be expressed in terms of the incident wave at the discontinuity, a^+, as

$$a^- = \left(\mathrm{r}\,\mathrm{e}^{\mathrm{i}\alpha} + \frac{t^2 R\,\mathrm{e}^{\mathrm{i}(2\beta+\theta)}}{1-rR\,e^{\mathrm{i}(\alpha+\theta)}}\right)a^+, \quad b^+ = \frac{t\,\mathrm{e}^{\mathrm{i}\beta}}{1-rR\,\mathrm{e}^{\mathrm{i}(\alpha+\theta)}}a^+, \tag{12a,b}$$

where $\theta = \varepsilon - 2kl$. Squaring and taking the modulus gives

$$\left|\frac{a^-}{a^+}\right|^2 = \frac{r^2 - 2Rr\left(r^2\cos(\alpha+\theta) - t^2\cos(2\beta-\alpha+\theta)\right) + R^2\left(t^4+r^4-2t^2r^2\cos 2(\alpha-\beta)\right)}{1+(rR)^2-2(rR)\cos(\alpha+\theta)},$$

$$\left|\frac{b^+}{a^+}\right|^2 = \frac{t^2}{1+(rR)^2-2rR\cos(\alpha+\theta)}. \tag{13a, b}$$

If the magnitude of the boundary reflection coefficient, R, is zero, i.e. the system can be considered semi-infinite, then Eqs. (13a,b) reduce to

$$\left|\frac{a^-}{a^+}\right|^2 = r^2, \quad \left|\frac{b^+}{a^+}\right|^2 = t^2. \tag{14a,b}$$

In this case, the ratios of the wave magnitudes give the magnitudes of the reflection and transmission coefficients directly.

However, even in the more general case, when the magnitude of the boundary reflection coefficient, R, is non-zero, some simplifications can be made. It can be seen that the squared magnitudes given in Eq. (13) are oscillatory in nature. For the case where the discontinuity and boundary reflection and transmission coefficients at D and C, respectively, are either constants or slowly varying functions of frequency, these oscillations are controlled by the parameter θ, and arise from multiple reflections of waves from the boundary at C. The effects of these multiple reflections can be substantially reduced by frequency averaging over a frequency range corresponding to $\theta = 2\pi$. After integration and some manipulation, Eqs. (13a,b)

then become

$$\overline{\left|\frac{a^-}{a^+}\right|^2} = \frac{1}{2\pi}\int_0^{2\pi}\left|\frac{a^-}{a^+}\right|^2 \mathrm{d}\theta = r^2 + \frac{R^2t^4}{1-(rR)^2},$$

$$\overline{\left|\frac{b^+}{a^+}\right|^2} = \frac{1}{2\pi}\int_0^{2\pi}\left|\frac{b^+}{a^+}\right|^2 \mathrm{d}\theta = \frac{t^2}{1-(rR)^2}. \tag{15a, b}$$

These estimates now more closely resemble the anechoic case given in Eq. (14). However, it should be noted that a bias has been introduced, with the results being overestimates of r^2 and t^2. For the case of small R, i.e. a weakly reflecting boundary, Eqs. (15a,b) can be expanded in powers of R. Neglecting terms of higher order than R^2 gives

$$\overline{\left|\frac{a^-}{a^+}\right|^2} = r^2\left(1 + \frac{t^2}{r^2}(tR)^2\right),$$

$$\overline{\left|\frac{b^+}{a^+}\right|^2} = t^2\left(1 + (rR)^2\right). \tag{16a, b}$$

2.2.1. Measurement considerations

From a measurement perspective, in order to determine the reflection and transmission properties of the discontinuity, the following steps would need to be performed: excitation of the structure; measurement of vibration at various locations within the structure; evaluation of wave amplitudes; and finally estimation of the reflection and transmission coefficients. In this symmetrical case, there are two unknown coefficients in Eq. (10). One set of wave measurements either side of the bend will result in the two simultaneous equations required to determine the two reflection and transmission coefficients. However, in two specific cases, the analysis can be simplified.

For the case when the waveguide B can be considered semi-infinite, Eqs. (14a,b) can be applied independently to the measured wave amplitudes and the magnitudes of the reflection and transmission coefficients found directly.

When the boundary at C is only weakly reflecting, Eqs. (15) and (16) may be used to estimate the magnitudes of the coefficients: the squared wave amplitude ratios are calculated as for the semi-infinite case, and then a moving average performed on the data over a frequency range corresponding to a phase change of $\theta = 2\pi$ at each frequency. In this case, an estimate of the error can then be made by calculating the magnitude of the residual terms in Eqs. (16a,b), proportional to R^2.

Here, a few points may be noted. For a conservative discontinuity, the magnitudes of the discontinuity reflection and transmission coefficients are related by

$$r^2 + t^2 = 1. \tag{17}$$

This means that, when the discontinuity reflection coefficient is small, the relative error in the estimate of the reflection coefficient as given by Eq. (16a) will be large, with the absolute error tending to R^2. In this case, the error in the estimate of the transmission coefficient as given by Eq. (16b) will tend to zero. If the discontinuity reflection coefficient is large (so that the transmission coefficient tends to zero), the error in the estimate of the reflection coefficient will also tend towards zero. (This is intuitively obvious as, if the discontinuity transmission coefficient is zero, there will be no reflections from the boundary of the system at C, as no waves will be transmitted into B.) Here, the relative error in the estimate of the transmission coefficient will tend to R^2.

In the following section, in order to demonstrate the procedure, it is applied to a beam undergoing flexural excitation.

3. Application to a beam undergoing flexural excitation

Flexural wave measurements were made on a beam with a discontinuity in order to demonstrate the possible approaches. The discontinuity comprised a mass and a moment of inertia. Measurements were made

sufficiently far from the discontinuity that nearfield waves could be ignored; moreover it was assumed that any axial motion was insignificant.

A simple model of the beam was developed for comparison with the measurements, in which the connection at the discontinuity was assumed to be a point one. The reflection and transmission matrices were found by considering continuity and equilibrium conditions.

3.1. Experimental setup and procedure

The experimental arrangement consisted of a 6 m length of rectangular section steel (50 mm × 6 mm), suspended freely, with a mass added approximately at its centre. The beam and added mass properties are shown in Table 1. In order to create the condition of weakly reflecting boundaries, the rig was configured so that it had flexural semi-anechoic terminations at each end. This was achieved by using foam wedges in sand boxes. The experimental arrangement is shown in Fig. 2.

Transducer pairs (spacing 20 mm) were located on either side of the discontinuity and a small shaker was used to excite the beam on one side. Measurements were made up to 3.2 kHz. From the measurements the amplitudes of the incident, reflected, transmitted and end-reflected waves were determined.

Having calculated the wave amplitudes, the magnitudes of the power reflection and transmission coefficients of the discontinuity were estimated using the three approaches described in the previous section: full matrix inversion; the assumption of anechoic boundaries; and the assumption of weakly reflecting boundaries. These were then compared with the theoretical predictions.

3.2. Determining the frequency range for averaging

In order to employ the averaging approach for weakly reflecting boundaries, it was first necessary to determine the averaging frequency range at each frequency. As the flexural waves are dispersive, this frequency range varies with frequency. From Eqs. (15a,b) the required range corresponds to a phase change of $\theta = 2\pi$ at each frequency, where $\theta = \varepsilon - 2kl$. Here, ε is the phase of the beam end reflection coefficient, k is the beam flexural wavenumber, and l is the distance from the discontinuity to the beam end. At any given frequency ω_0, corresponding to wavenumber k_0, averaging needs to take place over a wavenumber range

$$k_1 \leqslant k_0 \leqslant k_2, \text{ where } k_1 = k_0 - \frac{\pi}{2l} \text{ and } k_2 = k_0 + \frac{\pi}{2l}.$$

Table 1
Beam and added mass properties

Length (m)	6.0
Depth (m)	0.05
Thickness (m)	0.006
Elastic modulus (N/m^2)	1.94×10^{11}
Density (kg/m^3)	7800
Added mass (kg)	0.3127
Added rotational inertia (kg m^3)	2.071×10^{-4}

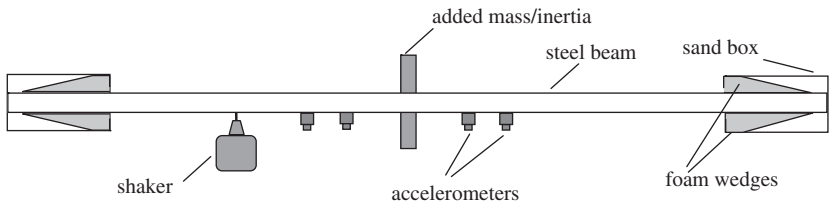

Fig. 2. Experimental arrangement for beam measurements.

For flexural waves for which $k \propto \omega^{1/2}$, the corresponding minimum and maximum frequencies ω_1 and ω_2 are given by

$$\omega_1 = \omega_0 \left(1 - \frac{\pi}{2k_0 l}\right)^2, \quad \omega_2 = \omega_0 \left(1 + \frac{\pi}{2k_0 l}\right)^2$$

giving a total frequency averaging bandwidth of $\omega_2 - \omega_2 = \omega_0 2\pi/k_0 l$ or $\Delta f = (\omega_2 - \omega_1)/2\pi = c_0/l$, where c_0 is the wavespeed at the frequency of interest.

It is interesting to note that this is twice the frequency range that would be applied if the waves were non-dispersive.

3.3. Experimental results

Figs. 3(a) and (b) show the three experimental estimates of the power reflection and transmission coefficients, along with the theoretical predictions. The figures show that, as expected, the assumption of anechoic boundaries produces results which are oscillatory, with the oscillations resulting from flexural waves being reflected from the beam end. For the reflection coefficient (Fig. 3(a)), full matrix inversion and the assumption of weakly reflecting boundaries produce smoother results which, in the mid-frequency range are very similar. At low frequencies, when the reflection coefficient is close to zero, the averaging results in an overestimate when compared with the full matrix inversion, as expected, due to the bias expressed in Eq. (16a). This was, as expected, found to be approximately equal to the square of the magnitude of the beam end reflection coefficient as estimated from the measured data (not shown). At high frequencies, the averaging produces a result which is smoother than the full matrix inversion estimate. For the transmission coefficient (Fig. 3(b)), again full matrix inversion and the assumption of weakly reflecting boundaries produce smoother results; in this case, however, using the averaging approach removes more of the oscillations at all frequencies. In addition, as expected, at all frequencies the bias error is small.

3.4. Comparison with theory

In general, the results compare well with the theoretical predictions. For both the reflection coefficient and the transmission coefficient, the overall trends have been reproduced for frequencies up to approximately 2500 Hz, and the absolute agreement is good. In the mid-frequency range, the measured reflection coefficients using the averaging procedure are slightly higher than the predictions, with the measured transmission coefficients being slightly lower. That these measurements compare well with the results using full matrix inversion suggest that, in this frequency regime, the differences compared with the predictions are not due to the averaging process as such, but probably due to modelling limitations. At higher frequencies, although the absolute agreement is still fair, the trends do not agree. Again, this is most likely to be due to limitations in the theoretical model; Euler–Bernoulli beam theory will still be valid at these frequencies, but elasticity effects in the discontinuity, which have not been considered (due to non-rigidity of the added mass and its connection to the beam), will start to have an impact. More sophisticated models are, of course, possible, but, in the authors' opinion, would not serve to illuminate the advantages of the proposed averaging procedure in this case any further.

4. Application to a right-angled bend in a pipe

In this section, the averaging process for weakly reflecting boundaries described in Section 2 is applied to measurements made on a right-angled bend in a pipe, undergoing excitation in the plane of the bend; the difference here is that more than one wavetype may be present; at low frequencies (below the cut-on frequency for the $n = 2$ ovalling mode), only axial and in-plane flexural waves are excited, although out-of-plane flexural and torsional waves can exist. In this case it is more difficult to measure and excite all the wavetypes and estimate the reflection and transmission coefficients using full matrix inversion. Furthermore, the inversion is

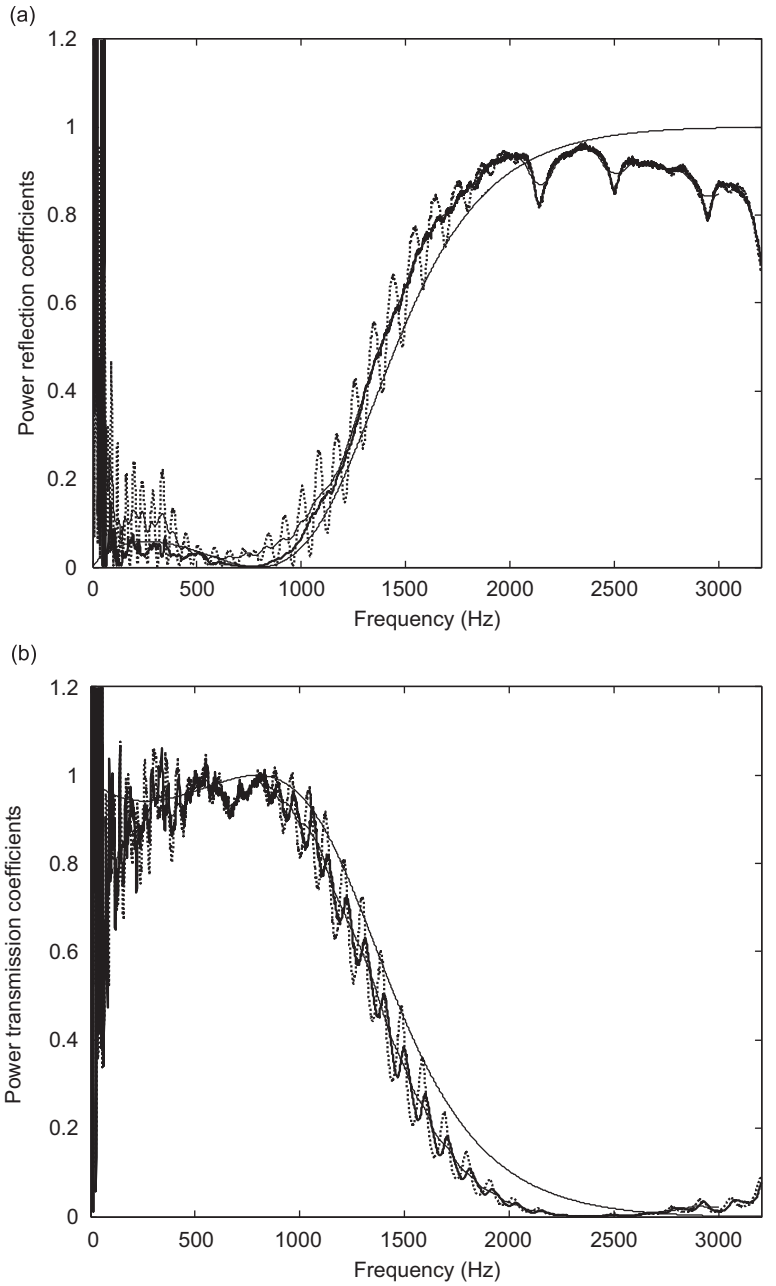

Fig. 3. Power coefficients for a beam with an added mass/moment of inertia discontinuity: (a) reflection coefficients and (b) transmission coefficients. Thick solid line: full matrix inversion; thick dotted line: anechoic assumption; thin solid line: assumption of weakly reflecting boundaries; thin dotted line: theoretical result.

prone to poor conditioning and hence numerical inaccuracies. Approximate methods therefore become of more interest.

4.1. Theoretical model of right-angled bend

As for the beam, a simple model of a pipe bend was developed for comparison with the measurements, in which the connection at the bend was assumed to be a rigid, massless, point connection [1,17]. The reflection

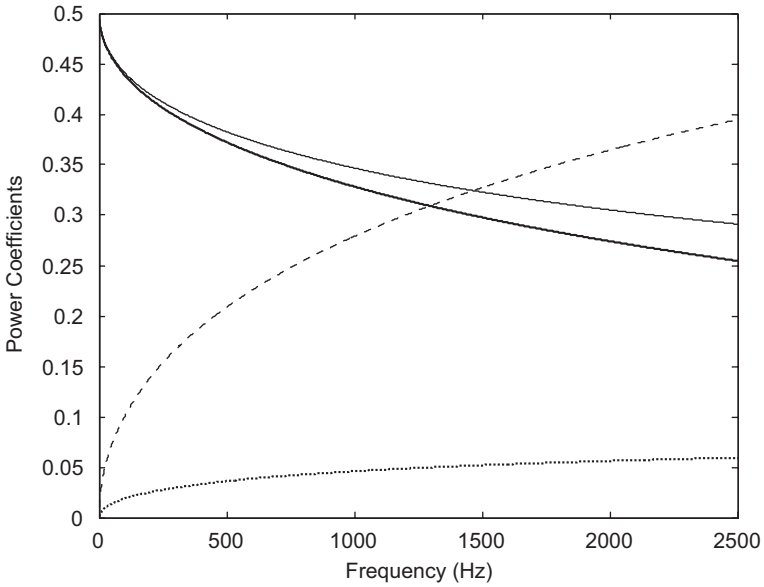

Fig. 4. Power reflection and transmission coefficients for an incident flexural wave. Thick solid line: reflected flexural; thick dotted line: reflected axial; thin solid line: transmitted flexural; and thin dotted line: transmitted axial.

and transmission matrices were found by considering continuity and equilibrium at the bend. The details of the model are not included here, but the power reflection and transmission coefficients for a flexural wave incident upon the discontinuity as predicted by the model are shown in Fig. 4. The dimensions and material properties of the modelled pipe are the same as those used in the experiments described in the following section.

4.2. Experimental setup and procedure

Measurements were taken on a right-angled pipe bend. The experimental arrangement consisted of two 4 m lengths of copper pipe (28 mm O/D, 0.9 mm wall thickness) connected together with a soldered 90° elbow, and suspended freely. In order to minimize unwanted reflections, the rig was configured so that it had both flexural and axial semi-anechoic terminations at each end. This was achieved by using foam wedges in sand boxes for the flexural waves and steel plates for the axial waves, a similar approach to that described previously by Brennan et al. [18], in which the thickness of the plate is chosen so that the characteristic impedance of the plate is equal to that for axial vibrations of the pipe, so the energy in the axial waves is transmitted effectively into the plate. The experimental arrangement is shown in Fig. 5.

An instrumented hammer was used to excite the pipe, and a number of different transducer configurations were used to make the measurements. As discussed earlier, only in-plane flexural waves and axial waves should be excited, so provision was made to measure these wavetypes only. In order to be able to determine these waves in both pipe arms simultaneously for one hammer hit, a large number of transducers would have been required. For practical reasons this was not possible, so for all the measurements, three pairs of accelerometers were used, located either side of the pipe, sufficiently far from the pipe ends, the pipe bend, and the excitation point, so that nearfield effects were negligible. Pairs were used to compensate for the fact that the transducers were not located on the neutral axis, with the outputs summed for the axial wave measurements and differenced for the flexural wave measurements; three sets (not equispaced for the flexural wave measurements) were used to decompose the waves, to avoid the singularity that is associated with a pair of transducers being spaced a half-wavelength (or an integer number of half-wavelengths) apart. The configurations allowed either the axial (accelerometers aligned axially) or the flexural (accelerometers aligned radially) waves in one arm of the pipe to be determined for any single hammer hit. It was anticipated that, by configuring the accelerometers in this way, axial motion would not significantly influence the flexural wave

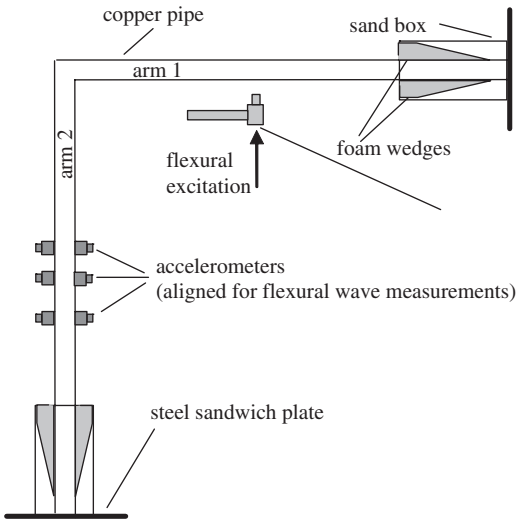

Fig. 5. Experimental arrangement for pipe measurements.

measurements and flexural motion would not significantly influence the axial wave measurements, so the wavetypes could be measured independently [19]. It was considered that the direction of the excitation was sufficiently repeatable to perform the measurements in this way; although the magnitudes of the impact varied between tests, this does not matter, as all the results were normalized by the input force. Tests were carried out exciting one arm of the pipe in flexure in order to determine the coefficients for incident flexural waves using the procedure for weakly reflecting boundaries. In this way, only one quarter of the full complement of measurements is required. Both flexural and axial wave measurements were made. Measurements were made up to 2.5 kHz, above which higher order pipe modes were seen to cut-on [20].

4.3. Experimental results

4.3.1. Flexural wave measurements

For the flexural wave measurements the transducers were spaced 20 and 30 cm apart (total 50 cm), thus allowing a least-squares wave decomposition to be undertaken using all three transducer pairs.

Fig. 6 shows the magnitude of the outgoing and returning flexural waves in each arm of the pipe, for flexural excitation. As expected, the wave with the largest amplitude is the incident wave in arm 1 (the excited arm) of the piping system; the wave with the next largest amplitude, as predicted by the model (Fig. 4), is the reflected flexural wave in arm 1; the end-reflected wave in arm 2 is the wave with the smallest amplitude. It is clear from the figure that the pipe ends were not completely anechoic for flexural waves: the end-reflected wave in arm 2 is not insignificant, and there are oscillations present in the magnitude of the incident wave in arm 1. However, at frequencies above about 500 Hz, the amplitude of the end-reflected wave in arm 2 is approximately one-tenth of the magnitude of the transmitted wave in arm 2, suggesting that the end reflection coefficient for flexural waves is small. Examination of the phase of the waves (not shown) revealed that each wave component was dominated by that which was expected at all frequencies up to 2500 Hz: the incident wave by a flexural wave travelling directly from the excitation point to the measurement location in arm 1; the reflected wave by a wave travelling from the excitation point to the bend and back to the measurement location in arm 1, all as a flexural wave; the transmitted wave by a wave travelling from the excitation point to the bend and on to the measurement location in arm 2, all as a flexural wave; and the end-reflected wave in arm 2 by a wave travelling from the excitation point to the bend, on to the 'end' of arm 2 and back to the measurement location in arm 2, all as a flexural wave. (The 'end' of the pipe, as determined by this predominant reflection was found, in fact, to be the front end of the sandbox, i.e. on first contact with the foam wedge.)

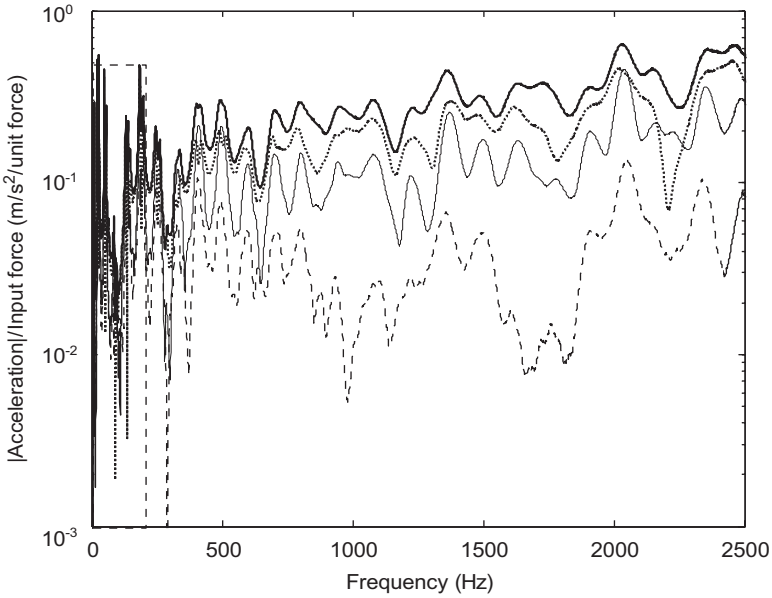

Fig. 6. Flexural wave amplitudes in each pipe arm; flexural excitation. Thick solid line: incident wave, arm 1; thick dotted line: reflected wave, arm 1; thin solid line: transmitted wave, arm 2; and thin dotted line: end-reflected wave, arm 2.

4.3.2. *Axial wave measurements*

For the axial wave measurements, the transducers were spaced 25 and 25 cm apart (total 50 cm), again allowing a least-squares wave decomposition to be undertaken using all three transducer pairs. The wavespeed for axial waves in this case was sufficiently high that no half-wavelength singularities were encountered in the frequency range of interest.

Fig. 7 depicts the magnitudes of the outgoing and returning axial waves in each arm of the pipe for flexural excitation. Here the wave with the largest amplitude is the wave transmitted into arm 2. This is as expected as the transmission coefficient for transmitted axial waves/incident flexural waves was found from the model to be sizeable (Fig. 4). The pipe ends are, in fact, not perfectly anechoic for axial waves as the end-reflected waves in both pipe arms are not insignificant. However, for the most part, above 500 Hz, they are small compared with the wave transmitted to arm 2 even if comparable in magnitude to the wave reflected from the pipe bend in arm 1. Examination of the phase of the waves revealed a number of interesting results. As expected, the transmitted wave in arm 2 was found to result from a wave having travelled from the excitation point to the bend as a flexural wave and then on to the measurement location in arm 2 as an axial wave. The reflected wave in arm 1 arose from a wave having travelled from the excitation point to the bend as a flexural wave and then back to the measurement location in arm 1 as an axial wave. Below 500 Hz, the phase of the end-reflected wave in arm 2 corresponded to a wave having travelled as a flexural wave from the excitation point, past the bend to the 'end' of arm 2 (the front of the sand box as before, for flexural waves) and then having been reflected from the pipe end back to the measurement location as an axial wave; above 500 Hz, its phase corresponded to a wave having travelled as a flexural wave from the excitation point to the bend and then as an axial wave to the 'end' of arm 2 (again the back of the sand box, for axial waves) and back to the measurement location. This is broadly in accordance with the model predictions: at low frequencies the model predicts that the flexural wave transmission coefficient for flexural waves incident on the bend is greater than the axial wave transmission coefficient for incident flexural waves; at higher frequencies, the reverse is true. It was not possible to infer the dominant path of the end-reflected wave in arm 1 with any certainty, but it did not seem to correspond to an axial wave propagating directly from the excitation location (i.e. any unintentional axial component in the hammer hit was small).

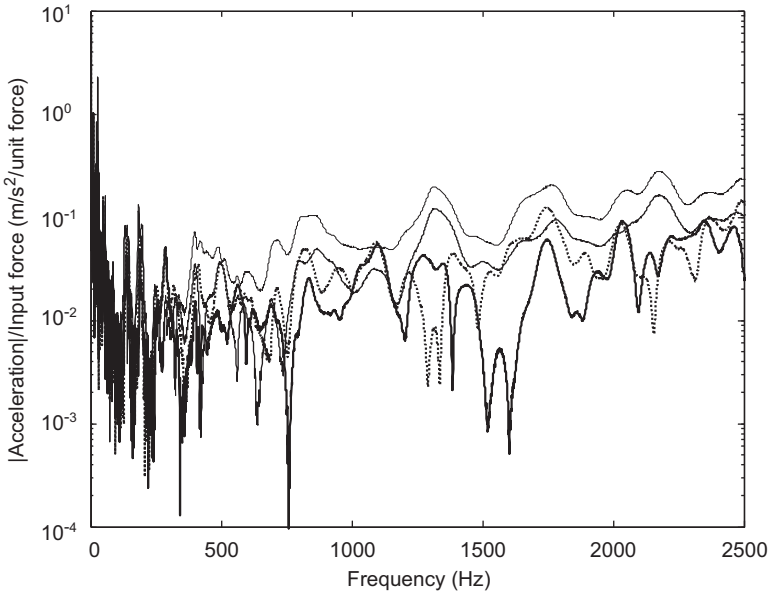

Fig. 7. Axial wave amplitudes in each pipe arm; flexural excitation. Thick solid line: end-reflected wave, arm 1; thick dotted line: reflected wave, arm 1; thin solid line: transmitted wave, arm 2; and thin dotted line: end-reflected wave, arm 2.

4.4. Determining the reflection and transmission coefficients

Having calculated the wave amplitudes, the power associated with each of the waves was calculated [3] and, as for the beam considered in Section 3, the magnitudes of the power reflection and transmission coefficients of the discontinuity (in this case the pipe bend) were estimated using the three approaches: full matrix inversion; the assumption of anechoic boundaries; and the assumption of weakly reflecting boundaries. In order to use the full matrix inversion technique, it was assumed that the discontinuity was symmetric, as described in Section 2.2; furthermore, data acquired previously from exciting the pipe axially [21] was used to supplement the data in order to attain the number of measurement sets required.

Inspection of the magnitude and phase of each the decomposed waves revealed that the assumption of weakly reflecting boundaries was reasonable: all the four waves scattered from the bend (reflected and transmitted flexural and axial waves) were dominated by the first arrival, as would be expected in this case. The results are shown in Figs. 8(a)–(d), along with the theoretical predictions. For light damping it does not matter that the measurement locations were some distance from the pipe bend rather than at the bend itself, as the decay in amplitude of the waves travelling over this distance will be negligible. For each of the coefficients, the averaging was performed on the basis that the first unwanted reflection (i.e. the lowest frequency of oscillation) arose from an axial wave being reflected from the pipe end; the frequency range over which a moving average was taken was therefore based on an axial wave having travelled twice the length of one pipe arm. As the axial waves are non-dispersive, this resulted in the averaging bandwidth being frequency-invariant and, in this case, equal to 424 Hz.

From the figures, a number of points can be noted. Assuming that the pipe ends are completely anechoic produces results which have large oscillations; the oscillations result from the unwanted reflections from the pipe ends, with higher frequency oscillations superimposed upon lower frequency ones. This is as expected, with the lowest frequency oscillation in most cases being associated with an axial wave being reflected from the pipe ends (peak spacing of around 424 Hz). Frequency averaging on this basis produces considerably smoothed results. For the axial waves (Figs. 8(c) and (d)), poor data at frequencies less than 500 Hz is responsible for the excessively large values in the averaged data at low frequencies. Full matrix inversion results in coefficients which are much less smooth, with very large peaks at some frequencies. This is because of poor conditioning and the effects of measurement noise, which make the results prone to error.

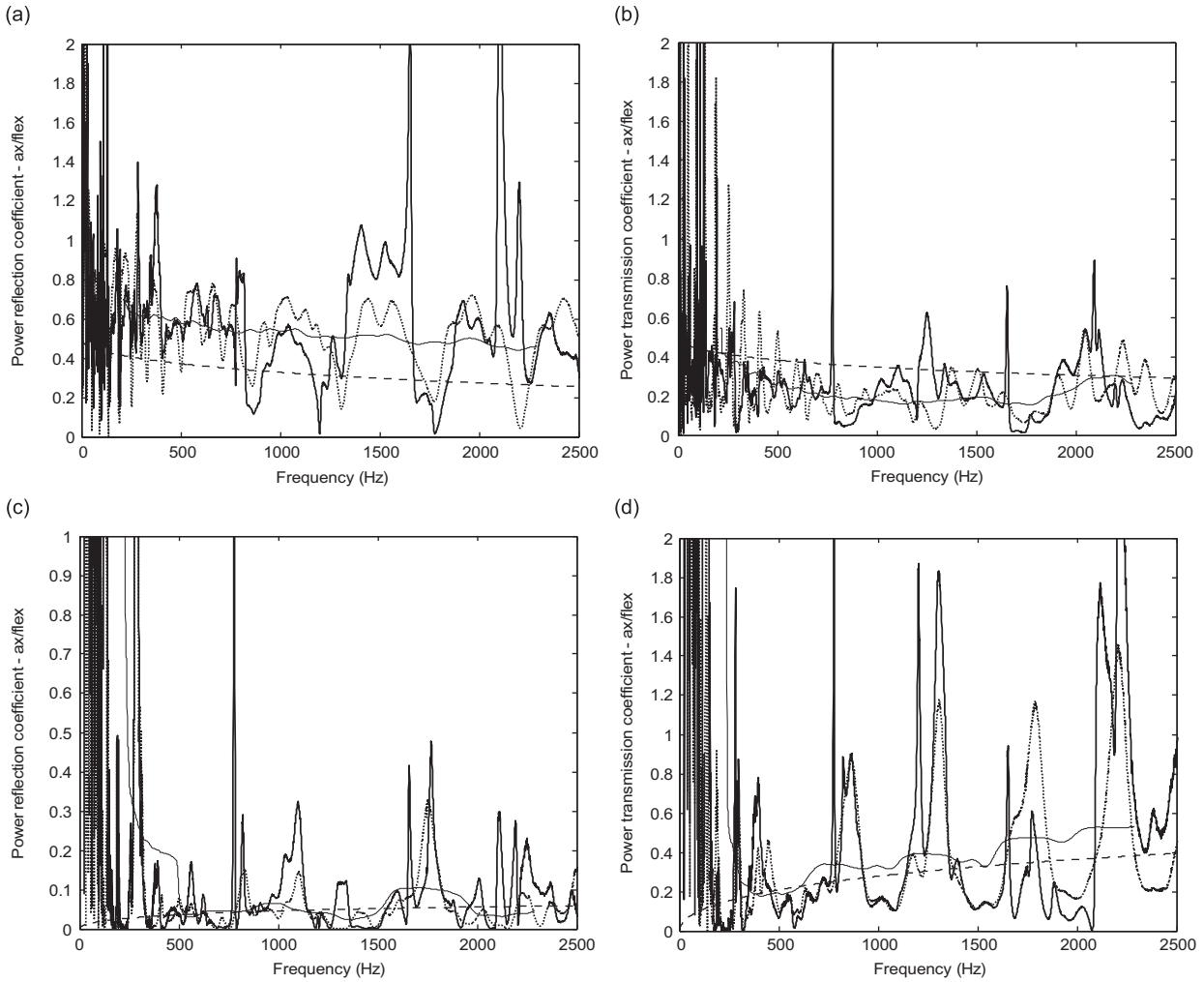

Fig. 8. Pipe bend power coefficients: (a) reflection coefficient—flexural/flexural; (b) transmission coefficient—flexural/flexural; (c) reflection coefficient—axial/flexural; and (d) transmission coefficient—axial/flexural. Thick solid line: full matrix inversion; thick dotted line: anechoic assumption; thin solid line: assumption of weakly reflecting boundaries; and thin dotted line: theoretical result.

Comparing the frequency averaged data with the theoretical results for the power coefficients, the overall trends have been reproduced for all the coefficients; for the axial wave coefficients, the absolute agreement is good for frequencies above 500 Hz; for the flexural wave coefficients, the absolute agreement is less good, with the reflection coefficient being larger than that predicted and the transmission coefficient being smaller.

There are a number of possible sources of experimental error, particularly at low frequencies. In analyzing the data in this way, it has been assumed that the waves incident on the bend in the excited arm contain only flexural components. It has been shown that this is not the case, and there is a significant axial component, particularly at frequencies lower than 500 Hz. As stated earlier, this does not seem to arise from unintentional axial excitation of the pipe, but more from unwanted axial reflections from the pipe end. That this effect is more significant at low frequencies is expected given that the effectiveness of the anechoic terminations will increase with increasing frequency. Eqs. (16a,b) show that the averaging process will always result in an overestimate of the required coefficient. If unwanted incident waves are also present, the estimate will be even more biased. However, Eqs. (16a,b) are only strictly valid when only one wavetype is present; when there are two wavetypes (as is the case here), the bias will increase and contain more terms with all four possible combinations of wave conversion boundary reflection coefficients. Estimates of the boundary reflection coefficients from the measured data indicate that the axial wave anechoic terminations, in particular, were not

as effective as hoped ($R^2 \sim 0.3$ for both flexural and axial reflected waves); these are likely to contribute to some bias error. At higher frequencies, comparison with the results obtained using full matrix inversion suggest that most of the difference between the measured data and the theoretical predictions is much more likely to be due to the limitations of the joint model. More sophisticated models are of course possible, for example in which the joint is considered to be finite [7], or in which mass and stiffness are added to the joint, but comparison with these is outside the scope of this paper.

5. Concluding remarks

In this paper, a number of approaches to measuring the reflection and transmission coefficients of a joint in a finite waveguide system have been described. In particular, an averaging procedure, which can be used when the boundaries of the system are weakly reflecting, is presented. The theoretical framework underpinning this procedure has been examined using a simple wave modelling approach, and the bias errors introduced when adopting this procedure revealed explicitly.

To illustrate the method, experiments were first conducted on a beam with a mass/moment of inertia discontinuity. In this case, only one wavetype was present. The reflection and transmission coefficients of the joint were determined using a full matrix inversion technique, assuming that there were no reflections from the boundaries, and finally using the proposed averaging procedure for weakly reflecting boundaries. The averaging procedure was found to reduce the effect of unwanted reflections considerably, with the results being as good as, if not superior to, those obtained using the full matrix inversion technique, once the expected bias was accounted for. Comparison with the theoretical results revealed some small differences, particularly at high frequencies, which were believed to be due to limitations of the model.

Experiments were then conducted on a pipe with a right-angled bend undergoing flexural excitation. Here, two wavetypes were present. Again, the reflection and transmission coefficients of the joint were determined using a full matrix inversion technique, assuming that there were no reflections from the pipe ends, and using the proposed averaging procedure for weakly reflecting boundaries. As for the beam, using the averaging procedure was found to be a significant improvement over assuming the boundaries to be completely anechoic, and in this case substantially better than using full matrix inversion. Exactly quantifying the bias error was not possible due to the presence of more than one wavetype but again, particularly at high frequencies, it was concluded that most of the error could be attributed to the limitations of the theoretical model.

To conclude, the proposed averaging approach, when appropriately applied, has significant advantages over acquiring a complete set of measurements and performing a full analysis: fewer measurements are required, and the results, being less susceptible to measurement errors, are likely to be smoother, and thus reveal the frequency trends more readily. Although a small bias error will remain, an estimate of this can be made and accounted for in the interpretation of the results.

Acknowledgement

The EPSRC are gratefully acknowledged for their support of this work.

References

[1] L. Cremer, M. Heckl, M.M. Ungar, *Structure-borne Sound*, Springer, Berlin, 1973.
[2] F.J. Fahy, E. Lindqvist, Wave propagation in damped, stiffened structures characteristic of ship construction, *Journal of Sound and Vibration* 45 (1976) 115–138.
[3] R.M. Grice, R.J. Pinnington, A method for the vibration analysis of built-up structures, part I: introduction and analytical analysis of the plate-stiffened beam, *Journal of Sound and Vibration* 230 (2000) 825–849.
[4] B.M. Gibbs, C.L.S. Gilford, The use of power flow methods for the assessment of sound transmission in building structures, *Journal of Sound and Vibration* 49 (1976) 267–286.
[5] R.A. Ibrahim, C.L. Pettit, Uncertainties and dynamic problems of bolted joints and other fasteners, *Journal of Sound and Vibration* 279 (2005) 857–936.

[6] H. Chebli, C. Soize, Experimental validation of a nonparametric probabilistic model of nonhomogeneous uncertainties for dynamical systems, *Journal of the Acoustical Society of America* 115 (2004) 697–705.
[7] B.R. Mace, Wave analysis of the T-beam, *Proceedings of the Internoise 97*, Budapest, 1997.
[8] C.R. Halkyard, B.R. Mace , Energy flow in a T-beam structure: measurement and modelling, *Proceedings of the Internoise 98*, Christchurch, New Zealand, 1998.
[9] M. Beshara, A.J. Keane, Vibrational energy flows in beam networks with compliant and dissipative joints, *Journal of Sound and Vibration* 203 (1997) 321–339.
[10] M.S. Ewing, S. Mirsafian, Forced vibration of two beams joined with a non-linear rotational joint: clamped and simply supported end conditions, *Journal of Sound and Vibration* 193 (1996) 483–496.
[11] H.Y. Hwang, Identification techniques of structure connection parameters using frequency response functions, *Journal of Sound and Vibration* 212 (1998) 469–479.
[12] J.H. Wang, S.C. Chang, Reducing errors in the identification of structural joint parameters using error functions, *Journal of Sound and Vibration* 273 (2004) 295–316.
[13] Y. Ren, C.F. Beards, Identification of joint properties of a structure using FRF data, *Journal of Sound and Vibration* 186 (1995) 567–587.
[14] F. Gautier, M.-H. Moulet, J.-C. Pascal, Reflection, transmission and coupling of longitudinal and flexural waves at beam junctions; part I: measurement methods, *Acta Acustica united with Acustica* 92 (2006) 982–997.
[15] M.-H. Moulet, F. Gautier, Reflection, transmission and coupling of longitudinal and flexural waves at beam junctions; part II: experimental and theoretical results, *Acta Acustica united with Acustica* 92 (2006) 1–11.
[16] B.R. Mace, Reciprocity, conservation of energy and some properties of reflection and transmission coefficients, *Journal of Sound and Vibration* 155 (1992) 375–381.
[17] B.M. Gibbs, J.D. Tattersall, Vibrational energy transmission and mode conversion at a corner-junction of square section rods, *Transactions of the ASME* 109 (1987) 348–355.
[18] M.J. Brennan, S.J. Elliott, R.J. Pinnington, The dynamic coupling between piezoceramic actuators and a beam, *Journal of the Acoustical Society of America* 102 (1997) 1931–1942.
[19] C.R. Halkyard, Sensor array design for wave decomposition in the presence of coupled motion, *Journal of Sound and Vibration* 259 (2003) 935–953.
[20] J.M. Muggleton, T.P. Waters, B.R. Mace, Measuring the reflection and transmission coefficients of joints in piping systems, *Recent Advances in Structural Dynamics*, Southampton, 2006.
[21] J.M. Muggleton, T.P. Waters, M.J. Brennan, Determining the dynamic properties of joints in piping systems, *Proceedings of the 2006 International Conference on Noise and Vibration Engineering*, 18–20 September 2006, Leuven, Belgium.